# An RC Load Model of Parallel and Series-Parallel Resonant DC–DC Converters with Capacitive Output Filter

Gregory Ivensky, Arkadiy Kats, and Sam Ben-Yaakov

*Abstract*— **A novel analytical methodology is proposed and applied to investigate the steady-state processes in voltage-fed parallel and series-parallel resonant dc–dc converters with a capacitive output filter. In this methodology, the rectifier, output capacitor, and load are replaced by an equivalent circuit which includes a capacitor and resistor connected in parallel. Excellent agreement was obtained when comparing numerical values calculated by the proposed model to cycle-by-cycle SPICE simulation and to the numerical results of earlier studies.**

*Index Terms*— **Approximate methods, circuit analysis, modeling, resonant power conversion.**

## I. Introduction

EXACT analysis of parallel and series-parallel dc–dc resonant converters with a capacitive output filter [1]–[3] is rather complex due to the fact that the equations include unknown time instances at which the output rectifier begins and ceases to conduct. The simplified analysis proposed by Steigerwald [4] is based on the method of the first harmonic. This approach is applicable to parallel and series-parallel converters with an $LC$ output filter, but does not cover the cases of a capacitor filter, in which the input current of the rectifier flows for only a part of the switching period.

The objectives of the present study are as follows:

1) to develop a simple analytical method for the analysis of parallel and series-parallel converters with a capacitive output filter (Fig. 1);
2) to obtain easy-to-use formulas and to apply them to develop design procedure for this class of converters.

## II. Main Equations Describing Steady-State Processes

The analysis was carried out under the following basic assumptions.

1) The converter's elements (switches, transformer, inductor, and capacitors) are ideal.
2) The reflected capacitance of the output filter $C_o$ and the capacitances of the input capacitors $C_{in}$ (in the case of half-bridge configuration) are much larger than the capacitances of series and parallel capacitors ($C_s$ and $C_p$).
3) The converter operates in continuous current mode.
4) The current $i_L$ of the resonant inductor $L_r$ (Fig. 2) can be approximated by

$$i_L = I_{Lm} \sin \vartheta \tag{1}$$

where $I_{Lm}$ is the peak value and $\vartheta = 2\pi f t$ is normalized time in radians with zero value at $\vartheta_o$ when the rectifier ceases to conduct, $f$ is the switching frequency, and $t$ is time. Experimental and simulation results obtained by Bhat [3] and by us confirm the practical validity of the last assumption.

The inductor current $i_L$ flows through the capacitor $C_p$ during the nonconducting interval of the rectifier $\vartheta_o$–$\vartheta_1$ and through the primary of the transformer $T$ during the conduct-

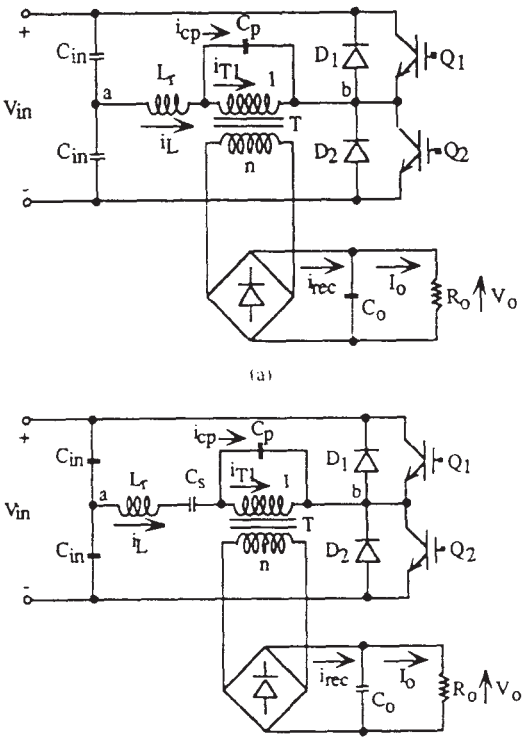


Fig. 1. Half-bridge configuration of (a) parallel and (b) series-parallel resonant dc–dc converters with capacitive output filter.

Manuscript received October 14, 1997; revised July 13, 1998. Recommended by Associate Editor, K. Ngo.

The authors are with the Power Electronics Laboratory, Department of Electrical and Computer Engineering, Ben Gurion University of the Negev, Beer-Sheva 84105, Israel (e-mail: sby@bguee.ee.bgu.ac.il).

Publisher Item Identifier S 0885-8993(99)03750-3.

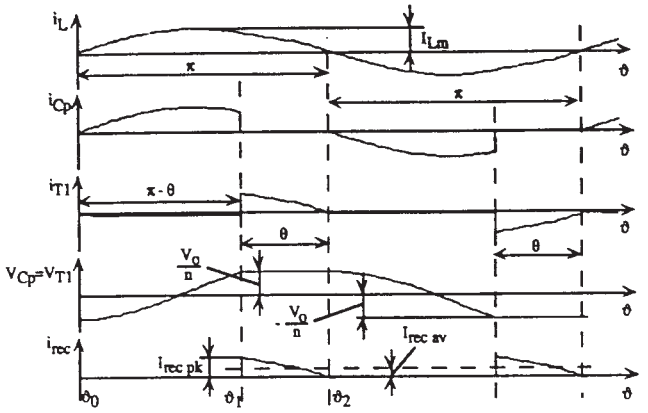


Fig. 2. Current and voltage waveforms.

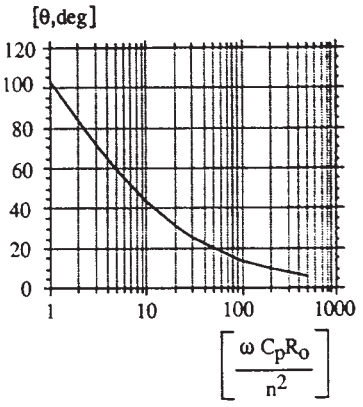


Fig. 3. Rectifier conduction angle $\theta$ as a function on the load coefficient $\omega C_p R_o/n^2$.

ing interval of the rectifier $\vartheta_1$–$\vartheta_2$. The rectifier's conduction angle $\vartheta_2$–$\vartheta_1$ is defined as $\theta$ (Fig. 2).

The voltage across the capacitor $C_p$ can be derived by applying the following initial conditions: at $\vartheta_0 = 0$ when the output rectifier ceases to conduct $v_{Cp} = -V_o/n$. At $\vartheta_1 = \pi - \theta$, when the output rectifier begins to conduct again, $v_{Cp} = V_o/n$, where $V_o$ is the output voltage and $n$ is the transformer's turns ratio (secondary to primary). Applying (1) along with the above boundary conditions, we get

$$v_{Cp} = \frac{V_o}{n(1+\cos\theta)}\left[(1-\cos\theta) - 2\cos\vartheta\right] \tag{2}$$

$$I_{Lm} = \frac{2V_o\omega C_p}{n(1+\cos\theta)} \tag{3}$$

where $\omega = 2\pi f$.

The output current of the converter $I_o$ is equal to the average rectifier's current $I_{rec\,av}$

$$\begin{aligned} I_o &= I_{rec\,av} \\ &= \frac{1}{\pi n}\int_{\pi-\theta}^{\pi} I_{Lm}\sin\vartheta\, d\vartheta \\ &= \frac{2}{\pi n} I_{Lm}\sin^2\left(\frac{\theta}{2}\right) \end{aligned} \tag{4}$$

or applying (3)

$$I_o = I_{rec\,av} = \frac{2}{\pi n^2} V_o\omega C_p \tan^2\left(\frac{\theta}{2}\right) \tag{5}$$

On the other hand

$$I_o = I_{rec\,av} = \frac{V_o}{R_o} \tag{6}$$

where $R_o$ is the load resistance.

From (5) and (6), we find the rectifier's conduction angle

$$\theta = 2\tan^{-1}\sqrt{\frac{\pi}{2}\frac{n^2}{\omega C_p R_o}}. \tag{7}$$

Relationship (7) is depicted in Fig. 3.

It should be noted that the voltage and especially the current waveforms of the transformer's primary $v_{T1}$ and $i_{T1}$ (Fig. 2) include high harmonics of significant amplitudes. However, the fact that the inductor current $i_L$, i.e., the current of the unbranched part of the ac circuit, has practically a sine waveform (see experimental results in [3]), only the fundamental harmonics of $v_{T1}$ and $i_{T1}$ will contribute to the output power of the converter. Consequently, an analysis based on fundamental harmonic approximation should provide a good approximation.

Now we find the first harmonics voltage and phase angle at the transformer's primary (Fig. 4). The primary transformer voltage $v_{T1}$ is the voltage $v_{Cp}$ across the capacitor $C_p$. Applying (2) and the condition that $v_{Cp}$ is equal to $V_o/n$ during the conduction interval of the rectifier, we find the peak value of the first harmonics of the primary transformer voltage

$$V_{T(1)m} = V_{Cp(1)m} = \frac{V_o}{n}k_v \tag{8}$$

where $k_v$ is the voltage waveform coefficient

$$k_v = \sqrt{a_{v(1)}^2 + b_{v(1)}^2} \tag{9}$$

and

$$\begin{aligned} a_{v(1)} = \frac{2}{\pi}\Bigg(&\frac{1}{1+\cos\theta}\Bigg[(1-\cos\theta)\sin\theta \\ &- \left(\pi - \theta - \frac{1}{2}\sin 2\theta\right)\Bigg] - \sin\theta\Bigg) \end{aligned} \tag{10}$$

$$b_{v(1)} = \frac{2}{\pi}(1-\cos\theta). \tag{11}$$

The relationship $k_v$ as a function of $\theta$ is depicted in Fig. 5 (solid curve). This can be approximated by

$$k_v = 1 + 0.27\sin\left(\frac{\theta}{2}\right) \tag{12}$$

(see the dashed curve in Fig. 5).

The phase angle of the first harmonics component of the transformer's voltage (refer to the instant $\vartheta_o$ in Fig. 4) will be

$$\xi_{v(1)} = \tan^{-1}\left(\frac{a_{v(1)}}{b_{v(1)}}\right). \tag{13}$$

Note that $\xi_{v(1)} < 0$ because $a_{v(1)} < 0$. The primary transformer current $i_{T1}$ is the current of the resonant inductor $L_r$ during the conduction interval of the rectifier and is zero when the rectifier does not conduct. Applying (1), we find the

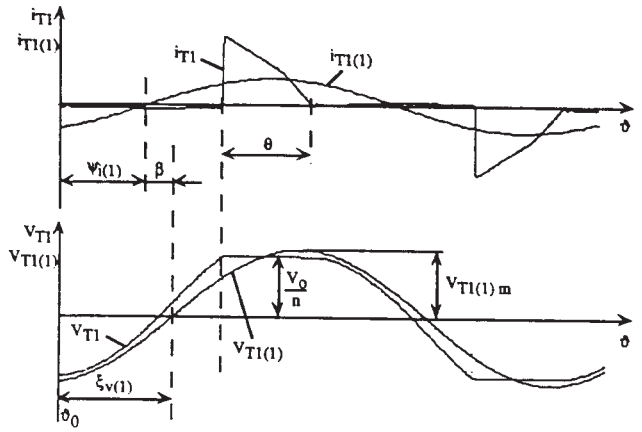


Fig. 4. The first harmonics of the current and voltage at the primary of the transformer.

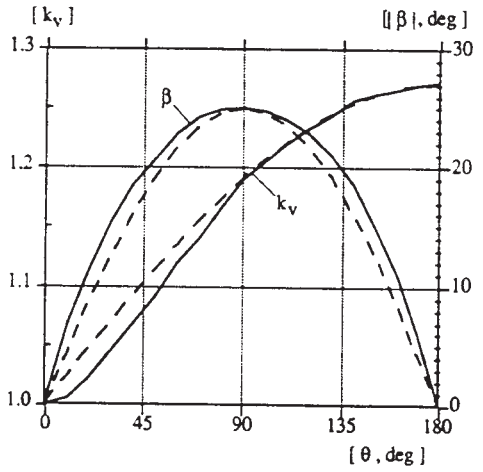


Fig. 5. The voltage waveform coefficient $k_v$ and phase angle $\beta$ versus the rectifier's conduction angle $\theta$; solid curves obtained by Fourier analysis; dashed curves—by approximate (12) and (16).

phase angle of the first harmonics transformer primary current (refer to the instant $\vartheta_o$ in Fig. 4)

$$\psi_{i(1)} = \tan^{-1}\left(-\frac{(1-\cos 2\theta)}{(2\theta - \sin 2\theta)}\right). \tag{14}$$

The difference

$$\beta = \xi_{v(1)} - \psi_{i(1)} \tag{15}$$

is the phase angle between the first harmonics of the primary transformer voltage and current (Fig. 4). The relationship $\beta$ as a function of $\theta$ calculated from (10), (11), (13), and (14) is depicted in Fig. 5 (solid curve). The graph can be described approximately by

$$\beta = -25 \sin \theta \text{ [deg]} \tag{16}$$

(see dashed curve in Fig. 5).

The fact that the angle $\beta$ is negative implies that the first harmonics of the primary transformer current $i_{T1(1)}$ lead the first harmonics of the primary transformer voltage $v_{T1}$. Hence, this analysis implies that the rectifier and capacitor filter load can be approximately represented by a

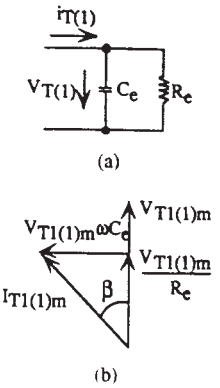


Fig. 6. Equivalent $R$–$C$ circuit replacing the (a) loaded transformer and (b) vector diagram of its voltage and currents.

resistive–capacitive ($R$–$C$) equivalent circuit such as shown in Fig. 6(a). In the case of a parallel-connected $R$–$C$ circuit [Fig. 6(a)], the equivalent resistor $R_e$ can be found from the relationship

$$\frac{V_o^2}{R_o} = \frac{V_{T(1)m}^2}{2R_e}. \tag{17}$$

Applying (8), we obtain

$$R_e = R_o \frac{k_v^2}{2n^2}. \tag{18}$$

The equivalent capacitance $C_e$ is found from [Fig. 6(b)]

$$\tan|\beta| = \omega C_e R_e. \tag{19}$$

Applying (18) and (19), we obtain

$$C_e = \frac{2n^2}{\omega R_o k_v^2} \tan|\beta|. \tag{20}$$

The peak value of the first harmonics of the primary transformer current can therefore be represented by

$$I_{T1(1)m} = \frac{V_{T(1)m}}{R_e \cos\beta} \tag{21}$$

or applying (6), (8), and (18)

$$I_{T1(1)m} = I_o \frac{2n}{k_v \cos\beta}. \tag{22}$$

The peak value of the first harmonics of the secondary transformer current will thus be

$$I_{T2(1)m} = \frac{I_{T1(1)m}}{n} = I_o \frac{2}{k_v \cos\beta}. \tag{23}$$

Applying the equivalent resistance $R_e$ and the equivalent capacitance $C_e$, the parallel and series-parallel converters with the capacitive output filter can be represented by the equivalent circuits of Fig. 7(a) and (b), respectively. $v_{ab}$ is the voltage between the points $a$ and $b$ of the original converters (Fig. 1). This voltage has a rectangular waveform with an amplitude of $\pm gV_{in}$, where $V_{in}$ is the converter input voltage and $g$ is topology constant ($g = 1$ in full bridge and $g = 0.5$ in half

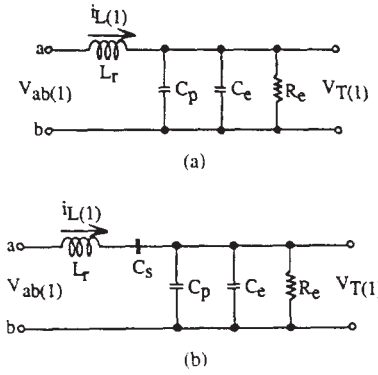


Fig. 7. Equivalent ac circuits of the (a) parallel and (b) series-parallel converter with capacitive output filter.

bridge). Hence, the peak value of the first harmonics of the voltage $v_{ab}$ can be found from

$$V_{ab(1)m} = \frac{4}{\pi} g V_{\text{in}}. \tag{24}$$

The expressions of the ac voltage ratio

$$k_{2-1} = \frac{V_{T(1)m}}{V_{ab(1)m}} \tag{25}$$

can be found by analyzing the equivalent circuits of Fig. 7.

For the parallel converter [Figs. 1(a) and 7(a)]

$$k_{2-1} = \frac{1}{\sqrt{\left[1 - \omega^2 L_r (C_p + C_e)\right]^2 + \left(\frac{\omega L_r}{R_e}\right)^2}} \tag{26}$$

or

$$k_{2-1} = \frac{1}{\sqrt{\left[1 - \left(\frac{\omega}{\omega_p}\right)^2 \left(1 + \frac{C_e}{C_p}\right)\right]^2 + \left[\left(\frac{\omega}{\omega_p}\right)^2 \frac{1}{\omega C_p R_e}\right]^2}} \tag{27}$$

where

$$\omega_p = \frac{1}{\sqrt{L_r C_p}}. \tag{28}$$

For the series-parallel converter [Figs. 1(b) and 7(b)], it is shown in (29) and (30), given at the bottom of the page, where

$$\omega_s = \frac{1}{\sqrt{L_r C_s}}. \tag{31}$$

The dc transformer ratio of the converter

$$V_o^* = \frac{V_o}{n g V_{\text{in}}} = \frac{V_o}{n V_{T(1)m}} \frac{V_{T(1)m}}{V_{ab(1)m}} \frac{V_{ab(1)m}}{g V_{\text{in}}} \tag{32}$$

or applying (8), (24), and (25)

$$V_o^* = \frac{4}{\pi} \frac{k_{2-1}}{k_v}. \tag{33}$$

Now we define the input phase angle $\varphi_{(1)}$, i.e., the angle between the voltage $v_{ab}$ and the first harmonics of the inductor $L_r$ current $i_{L(1)}$ (Fig. 7).

In the parallel converter [Figs. 1(a) and 7(a)]

$$\tan \varphi_{(1)} = \left(\frac{\omega}{\omega_p}\right)^2 \frac{1}{\omega C_p R_e} \{1 + [\omega(C_p + C_e)R_e]^2\} - \omega(C_p - C_e)R_e \tag{34}$$

where $R_e$ is equivalent load resistance [see (18)] and $C_e$ is equivalent capacitance [see (20)].

In the series-parallel converter [Figs. 1(b) and 7(b)]

$$\tan \varphi_{(1)} = \frac{1}{\omega C_p R_e} \frac{C_p}{C_s} \left\{ \left(\frac{\omega}{\omega_s}\right)^2 [1 - \omega^2 (C_p - C_e)^2 R_e^2] - 1 \right\} - [\omega(C_p - C_e)R_e] \left(1 + \frac{C_p - C_e}{C_s}\right). \tag{35}$$

Normalized output voltage $V_o^*$ and the input phase angle $\varphi_{(1)}$ versus normalized frequency ($\omega/\omega_p$ in parallel and $\omega/\omega_s$ in series-parallel converter) were calculated using the derived equations for different values of the quality factor

$$Q = \frac{\omega_p C_p R_e}{n^2}. \tag{36}$$

The results presented in Figs. 8 and 9 clearly show the resonant attributes of the converters.

For a sinusoidal inductor current (assumption 4), we obtain the following expressions for the average input current ($I_{\text{in av}}$) and for the average currents of the transistors and reverse diodes ($I_{Q\text{av}}$ and $I_{D\text{av}}$):

$$I_{\text{in av}} = \frac{2}{\pi} g I_{Lm} \cos \varphi_{(1)} \tag{37}$$

$$I_{Q\text{av}} = \frac{1}{\pi} I_{Lm} \cos^2 \left(\frac{\varphi_{(1)}}{2}\right) \tag{38}$$

$$I_{D\text{av}} = \frac{1}{\pi} I_{Lm} \sin^2 \left(\frac{\varphi_{(1)}}{2}\right) \tag{39}$$

$$k_{2-1} = \frac{1}{\sqrt{\left[1 + \frac{C_p + C_e}{C_s} - \omega^2 L_r (C_p + C_e)\right]^2 + \left(\omega L_r - \frac{1}{\omega C_s}\right)^2 \frac{1}{R_e^2}}} \tag{29}$$

or

$$k_{2-1} = \frac{1}{\sqrt{\left\{1 - \frac{C_p}{C_s}\left[\left(\frac{\omega}{\omega_s}\right)^2 - 1\right]\left(1 + \frac{C_e}{C_p}\right)\right\}^2 + \left\{\frac{C_p}{C_s}\left[\left(\frac{\omega}{\omega_s}\right)^2 - 1\right]\frac{1}{\omega C_p R_e}\right\}^2}} \tag{30}$$

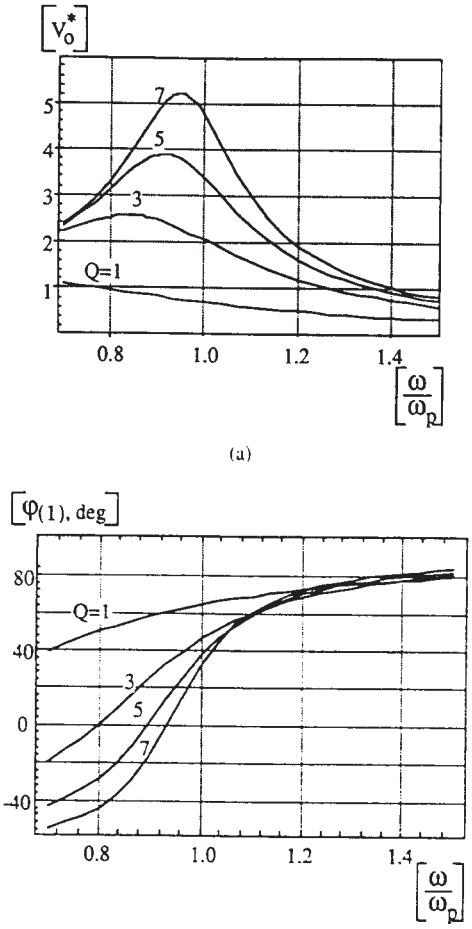


Fig. 8. (a) Normalized output voltage $V_o^*$ and (b) input phase angle $\varphi_{(1)}$ versus normalized frequency $\omega/\omega_p$ for different values of the quality factor $Q$; parallel converter.

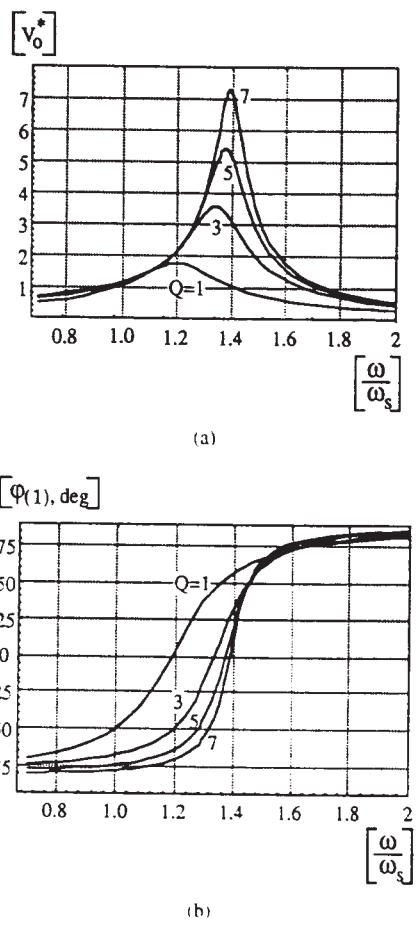


Fig. 9. (a) Normalized output voltage $V_o^*$ and (b) input phase angle $\varphi_{(1)}$ versus normalized frequency $\omega/\omega_s$ for different values of the quality factor $Q$; series-parallel converter when $C_s = C_p$.

or applying (37)

$$I^*_{Q\,av} = \frac{4gI_{Q\,av}}{I_{in\,av}} = \frac{1}{\cos\varphi_{(1)}} + 1 \tag{40}$$

$$I^*_{D\,av} = \frac{4gI_{D\,av}}{I_{in\,av}} = \frac{1}{\cos\varphi_{(1)}} - 1. \tag{41}$$

Equations (40) and (41) are plotted in Fig. 10 as a function of $\varphi_{(1)}$. The lowest values of these currents and therefore the lowest losses correspond to the case $\varphi_{(1)} = 0$.

Applying (4) and (37), we obtain

$$I_{in\,av} = ngI_o \frac{\cos\varphi_{(1)}}{\sin^2\left(\frac{\theta}{2}\right)}. \tag{42}$$

Neglecting losses (assumption 1)

$$\frac{I_{in\,av}}{I_o} = \frac{V_o}{V_{in}}. \tag{43}$$

Taking into account (42) and (43), we obtain an important expression of the output-to-input voltage ratio which can be useful in the design phase of the converter

$$V_o^* = \frac{V_o}{ngV_{in}} = \frac{\cos\varphi_{(1)}}{\sin^2\left(\frac{\theta}{2}\right)}. \tag{44}$$

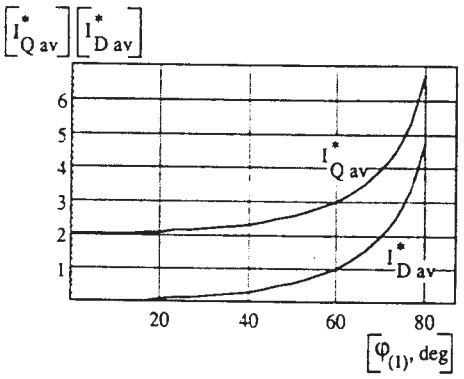


Fig. 10. Normalized average currents of the transistors ($I^*_{Q\,av}$) and reverse diodes ($I^*_{D\,av}$) as functions on the input phase angle $\varphi_{(1)}$ in parallel and series-parallel converters.

## III. Output Characteristics

Applying the per unit system, the base current unit is choosing to be as follows:

parallel converter [Figs. 1(a) and 7(a)]

$$I_{base} = \frac{gV_{in}}{n\sqrt{\frac{L_r}{C_p}}} \tag{45}$$

TABLE I
OUTPUT-TO-INPUT VOLTAGE RATIO ($V_o^*$) OF THE PARALLEL DC–DC CONVERTER WITHOUT TRANSFORMER COMPUTED BY PROPOSED METHOD AND BY STEIGERWALD [1]

| $\omega/\omega_p$ | $\omega C_p R_o \left(Q\frac{\omega}{\omega_p}\right)$ | $\theta$ [deg] eq.(7) | $k_v$ eq.(12) | $\beta$ [deg] eq.(16) | $\omega C_p R_e$ eq.(18) | $C_o/C_p$ eq.(20) | $k_{2\text{-}1}$ eq.(27) | $V_o^*$ eq.(33) | $V_o^*$ [1] |
|---|---|---|---|---|---|---|---|---|---|
| 0.700 | 1.594 | 89.6 | 1.190 | -25.0 | 1.129 | 0.413 | 1.880 | 2.0115 | 2.0 |
| 1.155 | 2.353 | 78.5 | 1.171 | -24.5 | 1.613 | 0.283 | 0.917 | 0.9970 | 1.0 |
| 0.940 | 6.369 | 52.9 | 1.120 | -19.3 | 3.988 | 0.0878 | 4.446 | 5.0540 | 5.0 |
| 0.940 | 3.622 | 66.7 | 1.148 | -23.0 | 2.387 | 0.178 | 2.685 | 2.9780 | 3.0 |
| 0.940 | 1.214 | 97.4 | 1.203 | -24.8 | 0.8785 | 0.526 | 0.9395 | 0.9944 | 1.0 |
| 0.940 | 0.6655 | 113.9 | 1.226 | -22.9 | 0.5001 | 0.845 | 0.5331 | 0.5536 | 0.5 |

and series-parallel converter [Figs. 1(b) and 7(b)]

$$I_{bas\,s} = \frac{gV_{in}}{n\sqrt{\frac{L_r}{C_s}}}. \tag{46}$$

Equations for the normalized average output current are obtained from (28), (31), (32), (36), (45), and (46) as follows:

parallel converter [Figs. 1(a) and 7(a)]

$$I_o^* = \frac{\frac{V_o}{R_o}}{I_{bas\,p}} = \frac{V_o^*}{Q} \tag{47}$$

and series-parallel converter [Figs. 1(b) and 7(b)]

$$I_o^* = \frac{\frac{V_o}{R_o}}{I_{bas\,s}} = \frac{V_o^*}{Q}\sqrt{\frac{C_p}{C_s}}. \tag{48}$$

Equations derived in Section II can be used for calculating the output voltage $V_o^*$ for given parameters of converter elements and given switching frequency (see Table I). The output current $I_o^*$ can be calculated after that from (47) or (48). The exception is short-circuit condition ($R_o = 0$) when the average output current $I_{o\,sh}^*$ must be found from other equations.

The parallel converter [Figs. 1(a) and 7(a)] (under assumption 4)

$$I_{o\,sh}^* = \frac{I_{o\,sh}}{I_{bas\,p}} = \frac{8}{\pi^2}\frac{\omega_p}{\omega} = 0.811\,\frac{\omega_p}{\omega}. \tag{49}$$

A more exact equation can be derived without the restriction of assumption 4

$$I_{o\,sh}^* = \frac{I_{o\,sh}}{I_{bas\,p}} = \frac{\pi}{4}\frac{\omega_p}{\omega} = 0.785\,\frac{\omega_p}{\omega}. \tag{50}$$

The series-parallel converter [Figs. 1(b) and 7(b)]

$$I_{o\,sh}^* = \frac{I_{o\,sh}}{I_{bas\,s}} = \frac{8}{\pi^2}\frac{1}{\left|\frac{\omega}{\omega_s} - \frac{\omega_s}{\omega}\right|}. \tag{51}$$

The equations derived above were applied to elucidate the output characteristics of the converters (Fig. 11, solid curves). The curves are in excellent agreement with simulation results obtained by our group (see the crosses and circles in Fig. 11). They also agree very well with the results of the complex analysis of Johnson and Erickson [2] and Bhat [3]. The output-to-input voltage ratios of the parallel converter calculated by the proposed method agree with the results of Steigerwald [1] to within 2% except for the very low $Q$ case (see Table I). Table I can be also used as a calculation guid. Note that the determination of output characteristics by the proposed method is much simpler than by more exact analyses [1]–[3]. This benefit is most important for circuit optimization for which the numerical data given in previous studies [1]–[3] may not

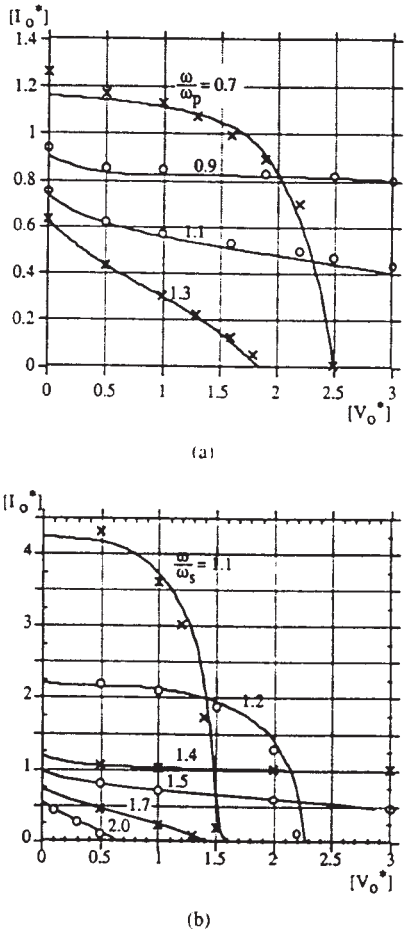


Fig. 11. The output characteristics of the (a) parallel converter and (b) series-parallel converter when $C_s = C_p$; solid curves obtained by calculation using the proposed method, with points (•) and (o) obtained by cycle-by-cycle simulation.

suffice. For example, in [3] the data for the series-parallel converter is given only for the case $C_s = C_p$.

## IV. Conclusions

The proposed equivalent circuit method simplifies the analysis and design of parallel and series-parallel resonant dc–dc converters loaded by a capacitive output filter. In contrast to previous, more exact numerical derivations, which were presented by tables and plots, the analytical relationships derived by the proposed method are more convenient as design tools and in particular for parameter optimization of these types of converters.

## References

[1] R. L. Steigerwald, "Analysis of a resonant transistor dc–dc converter with capacitive output filter," *IEEE Trans. Ind. Electron.*, vol. IE-32, pp. 439–444, Nov. 1985.

[2] S. D. Johnson and R. W. Erickson, "Steady-state analysis and design of the parallel resonant converter," *IEEE Trans. Power Electron.*, vol. 3, pp. 93–104, Jan. 1988.

[3] A. K. S. Bhat, "Analysis and design of a series-parallel resonant converter with capacitive output filter," *IEEE Trans. Ind. Applicat.*, vol. 27, pp. 523–530, May/June 1991.

[4] R. L. Steigerwald, "A comparison of half-bridge resonant converter topologies," *IEEE Trans. Power Electron.*, vol. 3, pp. 174–182, Apr. 1988.

**Gregory Ivensky** was born in Leningrad, USSR, in 1927. He received the Energy Engineer Diploma from the Leningrad Railway Transport Institute in 1948 and the Candidate and Doctor of Technical Sciences degrees from the Leningrad Polytechnic Institute in 1958 and 1977, respectively.

From 1951 to 1962, he was at the Central Design Bureau of Ultrasound and High Frequency Devices, Leningrad. From 1962 to 1989, he was at the Northwestern Polytechnic Institute, Leningrad, where in 1977 he became a Full Professor in the Department of Electronic Devices. Since 1991 he has been a Professor at the Department of Electrical and Computer Engineering, Ben-Gurion University of the Negev, Beer-Sheva, Israel. His research interests include power electronic systems such as high-power rectifiers and inverters, induction heating, and dc–dc converters.

**Arkadiy Kats** was born in Mariupol, Ukraine, in 1968. He received the B.Sc. degree in electrical engineering from Ben-Gurion University of the Negev Beer-Sheva, Israel, in 1995. He is currently workings towards the M.S. degree in electrical and computer engineering.

He carries out a research program at the Power Electronics Group of the Ben-Gurion University of the Negev Beer-Sheva. His fields of interest include dc/dc converter design and integrated magnetics.

**Sam Ben-Yaakov** was born in Tel Aviv, Israel, in 1939. He received the B.Sc. degree in electrical engineering from the Technion, Haifa, Israel, in 1961 and the M.S. and Ph.D. degrees in engineering from the University of California, Los Angeles, in 1967 and 1970, respectively.

He is presently a Professor at the Department of Electrical and Computer Engineering, Ben-Gurion University of the Negev, Beer-Sheva, Israel, and heads the Power Electronics Group there. He served as the Chairman of that department from 1985 to 1989. His current research interests include: power electronics, circuits and systems, electronic instrumentation, and engineering education. He also serves as a consultant to a number of commercial companies on various subjects including: analog circuit design, modeling and simulation, PWM and resonant converters and inverters, soft-switching techniques, and electronic ballasts for discharge lamps.